Natural and Anthropogenic Factors Controlling Circulation at the Terminus of a Seagrass-covered Estuary, Fort DeSoto Bay, West-Central Florida

Author(s): Charles G. Vickery, Ping Wang and Jun Cheng

Source: *Journal of Coastal Research*, July 2022, Vol. 38, No. 4 (July 2022), pp. 681-698

Published by: Coastal Education & Research Foundation, Inc.

Stable URL: https://www.jstor.org/stable/10.2307/48676908

Journal of Coastal Research	38	4	681–698	Coconut Creek, Florida	July 2022

Natural and Anthropogenic Factors Controlling Circulation at the Terminus of a Seagrass-covered Estuary, Fort DeSoto Bay, West-Central Florida

Charles G. Vickery, Ping Wang*, and Jun Cheng

School of Geosciences
University of South Florida
Tampa, FL 33620, U.S.A.

www.cerf-jcr.org

www.JCRonline.org

ABSTRACT

Vickery, C.G.; Wang, P., and Cheng, J., 2022. Natural and anthropogenic factors controlling circulation at the terminus of a seagrass-covered estuary, Fort DeSoto Bay, West-Central Florida. *Journal of Coastal Research,* 38(4), 681–698. Coconut Creek (Florida), ISSN 0749-0208.

Causeway construction and channel dredging are common engineering activities in shallow estuaries and can significantly alter natural circulation patterns. Bridges are often installed on causeways to improve circulation. This study examines the influence of dredged channels, causeways, and bridges on circulation patterns within a shallow estuary with dense seagrass beds using a calibrated and verified numerical model. For the case of Fort DeSoto Bay in west-central Florida, the causeways disrupted the natural east-west flow and reduced current velocities within the seagrass beds in the southern terminus portion of the estuary by up to 76%. The tidal bridges increased velocity in the stagnant areas by up to 226%. Up to 26% of the tidal prism in the lower half of the bay passes through the bridges during a spring flood-tidal cycle. Thus, the bridges significantly improved tidal flushing between the estuarine cells divided by causeways. The unvegetated dredged channels serve as efficient conduits that facilitate penetration of tidal currents into the southern and terminus of the bay, leading to significantly higher current velocity in the channels and corresponding reduced velocity over the adjacent seagrass beds. The channels allow for improved tidal flushing within the otherwise stagnant southern terminus of the bay and therefore can be designed for the purpose of improving circulation.

ADDITIONAL INDEX WORDS: *Estuary, Tampa Bay, tidal circulation, dredged channels, bridges, causeways, numerical modeling.*

INTRODUCTION

Seagrasses are among the most productive yet threatened ecosystems on earth (Van Katwijk *et al*., 2016). They have long been recognized for their role in providing refuge and nursery for marine organisms (Heck, Nadeau, and Thomas, 1997), enhancing water quality (Terrados and Borum, 2004), cycling nutrients (Flindt *et al.,* 1999), sequestering atmospheric carbon dioxide (Moki *et al*., 2020), and resisting the erosive effects of storm surges (Hansen and Reidenbach, 2012). Being tidally influenced systems, shallow estuaries are strongly reliant on tidal flushing to mediate a variety of physical, chemical, and biological processes (Walter, Rainville, and O'Leary, 2018). Anthropogenic modifications can alter natural circulation patterns and influence key water-quality parameters affecting seagrass health, such as temperature, dissolved oxygen, and salinity. Habitat fragmentation from poorly planned infrastructure activities, *e.g*., causeway construction, can compartmentalize an estuary and restrict the movement of transient estuarine species, reduce the reproductive success of salt-tolerant vegetation, and lower the overall biodiversity of the estuarine ecosystem (Brockmeyer *et al*., 1997; Erftemeijer and Lewis, 2006; Rose, 2008). For these reasons, adequate and efficient hydrodynamic circulation is a critical factor to consider when developing estuarine habitat rehabilitation strategies.

Seagrass beds can have a significant effect on tidal flow and wave propagation by influencing bottom friction. Peterson *et al*. (2004) and Moki *et al*. (2020) found that seagrasses in shallow estuaries exert a frictional force on the flow field that can influence large-scale circulation patterns. Fonseca and Fisher (1986) found that *Thalassia testudinum*, a seagrass species common to many Florida estuaries, generates the greatest flow retardance of all the common tropical seagrass species. Therefore, the loss of *T. testudinum* due to water-quality impairment, dredging, and propeller scarring can modify hydrodynamics and lead to resuspension of sediments (Hansen and Reidenbach, 2012). Modeling studies in Tampa Bay by Zervas and Bourgerie (1993) showed that current velocities are stronger in natural or dredged channels devoid of seagrasses when compared to shallower vegetated areas. Hansen and Reidenbach (2012) suggested that filling and revegetating dredged channels with native seagrasses can make estuaries more resistant to the effects of coastal erosion because the creation of seagrass beds has been shown to attenuate wave energy and to reduce sediment resuspension.

Construction of causeways across shallow estuaries was a common practice in the greater Tampa Bay area and many other estuaries before the 1970s (Goodwin, 1987). Impermeable causeways bisect estuaries and restrict tidal circulation. Their negative hydrodynamic and ecological effects can be mitigated by installing tidal bridges, viaducts, or culverts to facilitate water exchange and to improve habitat quality in poorly

DOI: 10.2112/JCOASTRES-D-21-00165.1 received 29 December 2021; accepted in revision 28 February 2022; corrected proofs received 4 April 2022; published pre-print online 27 April 2022.
*Corresponding author: pwang@usf.edu

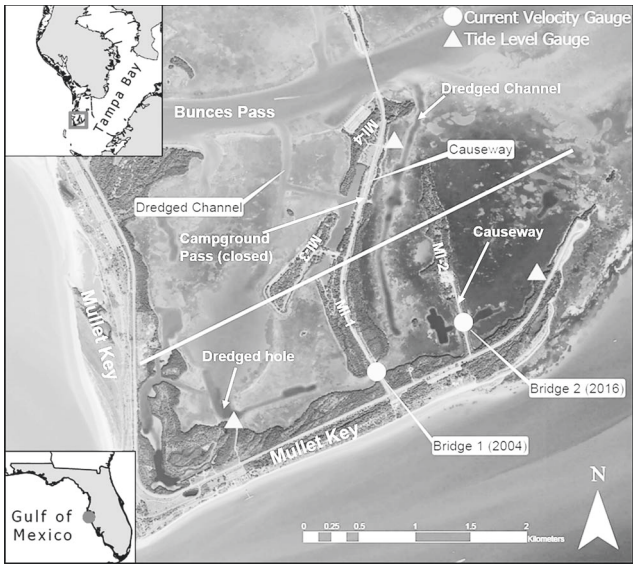

Figure 1. The Fort DeSoto Bay located at the mouth of Tampa Bay (top left inset) in west-central Florida (bottom left inset). Locations of water level and current velocity measurements are indicated. Key features are labeled (MI denotes Mangrove Island). The line in the middle separates the upper bay and lower bay. This line is drawn somewhat subjectively. Middle bay refers to the portion of the bay in the vicinity of the line and overlaps with upper and lower bay. The terms upper bay, middle bay, and lower bay are used generally for the convenience of discussion. The background aerial photo was taken in 2020, obtained from Google Earth.

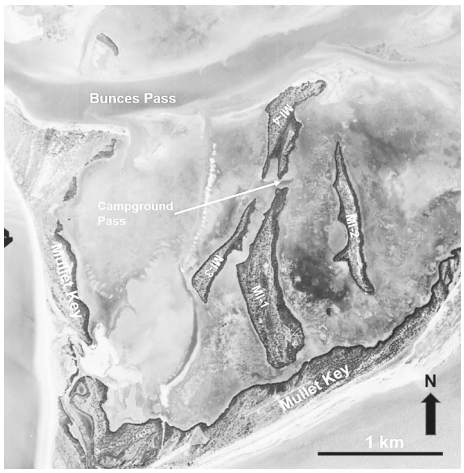

Figure 2. The Fort DeSoto Bay in 1943, before the significant anthropogenic activities. Some initial anthropogenic activities can be seen.

circulated areas. Pickering *et al*. (2018) have suggested that estuarine areas in the vicinity of bridges exhibit more natural flow regimes as compared with causeways. Brockmeyer *et al*. (1997) and Rose (2008) showed that culverts can improve water quality, increase fish production, and restore salt-tolerant vegetation in degraded areas. Raulerson *et al*. (2019) found that isolated dredge holes can serve as sinks for anthropogenic contaminants, such as pesticides and heavy metals; therefore, filling and revegetating these areas may help to improve water quality and ecological health.

Tidal circulation within the terminus of an estuary is often in limited simply due to its distal location from tidal inlets. However, because of its close proximity to land, this region is often subject to intense anthropogenic alterations. The delicate balance between hydrodynamics, water quality, and ecosystem health can be easily upset by poorly planned engineering activities. A common example is construction of causeways and subsequent compartmentalization of shallow estuaries. Fort DeSoto Bay, a small and shallow estuary within Tampa Bay, provides an insightful case study to examine the various natural and artificial factors influencing tidal driven circulation within the terminus of an estuary.

This study aims to comprehensively evaluate the influence of dredged channels, seagrass beds, causeways, dredge holes, and tidal bridges on circulation patterns in the shallow Fort DeSoto Bay. The Coastal Modeling System (CMS; Sanchez, Wu, and Beck, 2016; Sanchez *et al*., 2011, 2014), specifically the CMS-Flow, which was developed by the U.S. Army Corps of Engineers, was used to simulate the tidal driven circulation within Fort DeSoto Bay. The two-dimensional depth-averaged CMS-Flow model provides a suitable tool for simulating the flow patterns within this shallow estuary. The CMS-Flow model was calibrated and verified with *in situ* field measurements. The CMS-Flow model allows for the manipulation of environmental conditions, such as water depth, bottom friction, and layout of landforms, thus providing a valuable tool for simulating hydrodynamic response of future restoration efforts, such as tidal bridge constructions or dredged channel modifications. The numerical model was used to examine the influence of various natural and artificial factors on tidal flow patterns within the study area.

Study Area

Fort DeSoto Bay is a shallow estuary located landward of Mullet Key at the mouth of Tampa Bay in west-central Florida (Figure 1). The estuary is separated from the open sea by Mullet Key, a hook-shaped barrier island at the mouth of Tampa Bay. It is connected to the Gulf of Mexico via the Bunces Pass inlet channel to the north and the greater Tampa Bay to the east (Beck and Wang, 2019). Fort DeSoto Bay, as part of a County Park and a nature preserve, harbors an abundance of marine life, birds, mangroves, as well as the most extensive seagrass beds in Tampa Bay (Tomasko, 2000). The area has become the focus of numerous environmental restoration efforts because of its ecological value and importance as a popular community recreational area.

Before the passage of restrictive environmental regulations in the early 1970s, Fort DeSoto Bay experienced various anthropogenic alterations typical of many shallow estuaries, such as dredging and construction of causeways. These alterations are apparent when comparing the aerial photo of 1943 (Figure 2) before major human development with that of today (Figure 1).

Anthropogenic alteration intensified in the 1950s and 1960s in this area. Between 1951 and 1962, two causeways were

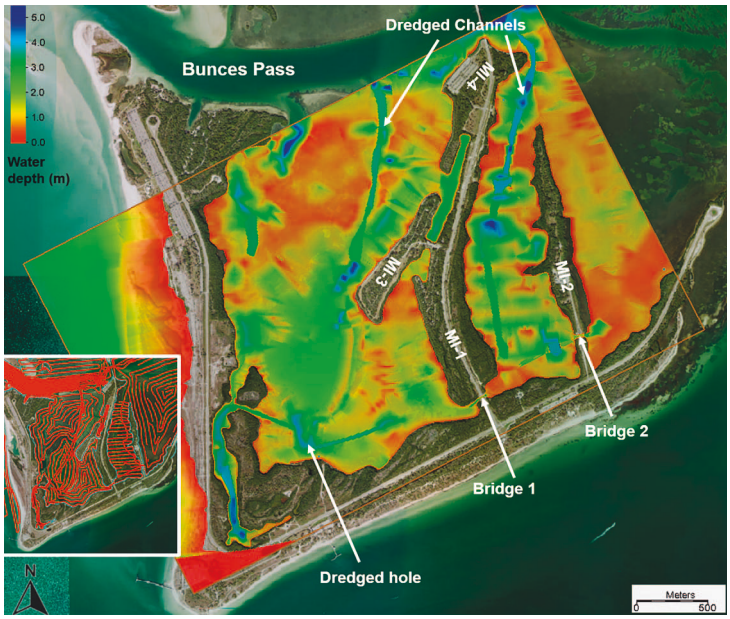

Figure 3. The complicated anthropogenically altered bathymetry of Fort DeSoto Bay captured by the dense survey coverage (left inset). The bathymetry is illustrated as water depth in meters relative to mean sea level. Key features are labeled.

constructed in the estuary (Figure 1). The long causeway to the west extending through two mangrove islands (Figure 1, MI1 and MI4) connected Mullet Key to the mainland. A large mangrove island (Figure 1, MI3) was converted to a popular campground and was connected to the long causeway through a short section of fill. The shorter causeway to the east connected a mangrove island (Figure 1, MI2) to the south shore. The mangrove island (Figure 1, MI2) was converted to a maintenance area for this popular County Park. Channels were dredged parallel to the long causeway to conveniently provide material for its construction. The dredged feature near the eastern causeway was excavated for construction material. A large and deep dredged hole (Figure 1) was excavated to provide additional construction material (Raulerson *et al.,* 2019). The combination of dredging and filling altered the bathymetric characteristics of the bay.

The north-south–trending causeways crossed regions of the bay that were previously open water between mangrove islands, which obstructed east-west tidal flow. The stagnation of water led to elevated water temperatures and reduced dissolved oxygen levels, causing severe stress and mortality of seagrass beds. These effects were most severe in the southern terminus of the estuary (SWFWMD, 2018). To improve/restore east-west tidal flow in the lower bay, a pair of 12-m-span bridges were installed on each causeway in 2004 and 2016, respectively. The two bridges are referred to in this study as Bridge 1 to the west (constructed in 2004) and Bridge 2 to the east (installed in 2016; Figure 1).

In addition to the circulation bridges, the Tampa Bay Estuary Program has identified a 4.26-m-deep (14-ft-deep) largely isolated dredge hole in the SW corner of the bay (Figure 1) for future complete or partial filling to reduce the severity of hypoxia and improve benthic habitat (Raulerson *et al.,* 2019). Filling and revegetating of isolated dredge holes may influence circulation patterns by reducing cross-sectional area and increasing frictional forces.

METHODS

This section describes the methods used to construct, calibrate, and verify the CMS-Flow model. A series of field measurements was conducted to ensure accurate representation of bathymetry of this shallow seagrass estuary. *In situ* measurements of tidal water-level fluctuations and flow velocities at the bridges were conducted to calibrate and verify the numerical model. Once the model was successfully verified, various scenarios were simulated to examine the factors influencing the tidal circulation within Fort DeSoto Bay.

Field Data Collection

The field data collection was designed with the overall goal of constructing an accurate numerical model of Fort DeSoto Bay. Data were collected over a 6-week period from 8 August to 18 September 2019 (three spring-neap tidal cycles) to measure flow velocities at the two bridges and tidal water-level fluctuations at strategic locations within the bay. Because the spans at both bridges are only 12 m, the numerical model should have small grid size to adequately resolve the bridge openings and the flow patterns through them. The tidal water-level measurement locations (Figure 1) were designed such that a small modeling domain can be defined.

Detailed bathymetry was surveyed using a vessel-mounted precision echo sounder (Teledyne Odom Hydrographic Echotrac CV100 single beam) synchronized with an RTK-GPS (Trimble R8s) system (Figure 3). Additional water depth data were collected in the vicinity of the bridge openings and under

the bridge using a Topcon Electronic Total Station following level-and-transit survey procedures. The cross-sectional area is accurately captured in the model based on the detailed survey because it has substantial control on the computed velocity. In addition, recent aerial photos (Figure 1) were used to ensure that the dredged channels are properly interpreted from the bathymetry data. Some additional bathymetry data points were added based on the aerial photos to ensure that the channels are correctly defined.

Tidal water-level fluctuations were collected at five locations within the shallow bay (Figure 1), including at the two bridges and boundaries to define the modeling domain. The tidal-driven flow velocities were computed based on the measured water-level fluctuations at the boundaries. Flow velocities were measured at the two bridge openings using Sontek Acoustic Doppler Velocimeters (ADVs). The water depth at bridges ranges from 0.6 to 1.6 m as controlled by tidal water level. The current meters were installed at roughly 0.45 m above seabed and should provide reasonable measurement of depth-average velocities. Measured flow velocities constitute the main data for model calibration and verification. Short-term flow measurements were also conducted at various locations near the numerical model boundaries using a portable current meter (Nortek Vector ADV) with the goal of identifying any potential significant flow conduits; however, none were identified.

Model Setup and Calibration

The CMS model has been successfully applied to various barrier-inlet systems along the west-central Florida coast (Beck and Wang, 2019; Beck *et al*., 2020; Wang and Beck, 2012; Wang, Beck, and Roberts, 2011). As discussed previously, the main goal of this study is to investigate the various natural and artificial factors that influence flow patterns in Fort DeSoto Bay using a numerical model. The considerations for defining the modeling domain and determining the size of the modeling grid were twofold: The modeling domain must be large enough to encompass the entire area of the Bay (Figure 1), and the grid cells must be small enough to provide for adequate spatial resolution of the various features, *e.g.,* the bridge openings and the dredged channels. The model grid size ranged from 8×8 m in the estuary interior, to 2×2 m in the vicinity of the bridges. This telescoping grid allows for fine spatial resolution of key features without compromising the model's overall efficiency. Figure 3 shows that the complicated bathymetry is well represented by the model. The flow simulation was driven by measured tidal fluctuations during a 6-week duration. Wind forcing was inherently included in the measured tides, although it did not represent a large range of conditions. The present model domain is too small for proper computation of wind forcing. It is beyond the scope of this paper to examine flow patterns under extreme weather conditions.

The numerical model was calibrated by comparing measured velocity values to the modeled values at the two bridges. Friction coefficient was the only parameter used in the calibration. A large portion of studied shallow estuary (Figure 1) is covered by seagrass beds, so it is crucial that their influence on flow field be properly represented. Current-wave interaction with seagrass beds has been the subject of numerous studies (Abdelrhman, 2003; Bryan *et al*., 2007; El Allaoui *et al*., 2016; Fonseca and Fisher, 1986; Hansen and Reidenbach, 2012; Le Bouteiller and Venditti, 2015, 2014; Moki *et al*., 2020; Paquier *et al*., 2020; Peterson *et al*., 2004). All these studies have suggested that seagrass beds would exert stronger friction forcing than barren surface. It is therefore reasonable to apply a larger friction coefficient, the Manning's roughness coefficient n in this case, for seagrass beds as compared with barren bed during the calibration process. Model calibration and selection of friction coefficients are discussed in the following. The bathymetry data and aerial photography were used to identify areas that are covered by seagrass beds. The Willmott (1981) skill (Equation [1]) was used to compare modeled to measured current velocities:

$$S_w = 1 - \frac{\sum (V_{model} - V_{measure})^2}{\sum \left(|V_{model} - \overline{V_{measure}}| + |V_{model} - \overline{V_{model}}| \right)} \quad (1)$$

where, S_w values closer to one signify less deviation between modeled and measured values and, therefore, a better model skill.

Tidal Prism Analysis

The overall influence of the two bridges on the water exchange was evaluated by computing the discharges through them and comparing to the tidal prism of the entire Fort DeSoto Bay. Tidal prism represents the total volume of water that flows into or out of an estuary between a high tide and the subsequent low tide (Dyer, 1997). The tidal prism (P) for a single tidal cycle can be calculated as:

$$P = \Delta H \cdot S \quad (2)$$

where, ΔH = tidal range and S = surface area of the estuary averaged over the tidal cycle (Fang, Xie, and Cui, 2015). For this study, the surface area of the Fort DeSoto Bay is somewhat subjectively defined as the model domain (Figure 3). To evaluate the contributions of the bridges to the southern portion of the bay, a lower bay was defined (Figure 1).

Volumetric discharge (Q) at each bridge was calculated based on the measured cross-sectional area of the openings and computed flow velocity as:

$$Q = \sum_t \sum_A \vec{v} \Delta A \Delta t \quad (3)$$

where, v = the computed depth-averaged velocity, ΔA is the cross-sectional area of the grid cell, and Δt is the time over which the discharge is computed. The discharge was summed across the entire cross-sectional area (A) under the bridge.

The computed discharge through the bridge (Equation [3]) is compared with the total tidal prism (Equation [2]) for the same period to determine what percentage of the total estuarine water volume flows through the two bridges. Because circulation is more restricted in the lower portion of the bay, a secondary tidal prism was calculated specifically for the lower bay (Figure 1) to better understand the contributions of the bridges.

Modeling Scenarios

A total of 10 scenarios were simulated to isolate and examine the effect of various factors on circulation patterns within Fort DeSoto Bay (Table 1). The first four modeling scenarios are

Table 1. *Summary of modeling scenarios.*

Scenario	Description
Actual 1 (A1)	Conditions prior to installation of the circulation bridge (before 2004)
Actual 2 (A2)	Existing conditions
Actual 3 (A3)	Predevelopment, *i.e.* natural conditions (before 1943)
Actual 4 (A4)	Conditions prior to Bridge 2 installation (between 2004 and 2016)
Hypothetical 1 (H1)	Bridges closed and dredged channels filled
Hypothetical 2 (H2)	Opening of new circulation bridge near the Fort DeSoto Campground
Hypothetical 3 (H3)	Filling of a large dredged hole in the SW corner of the bay
Hypothetical 4 (H4)	Closing of dredged channels
Hypothetical 5 (H5)	Closing of dredged channels/dredged holes, and reopening of Campground Pass
Hypothetical 6 (H6)	Closing of Bridge 1

based on actual conditions during different periods in history, such as the predevelopment conditions, whereas the remaining six cases represent hypothetical configurations. Scenarios H2 and H3 simulate potential restoration options with the goal of restoring to predevelopment conditions (Figure 2). The predevelopment scenario (A3) serves as a basis of comparison to evaluate how the tidal-driven circulation pattern was modified by the various engineering activities that were commonly applied to shallow estuaries.

RESULTS

This section presents the results of this study. Model calibration and verification are discussed first. Contribution of the bridges to the water budget in Fort DeSoto Bay, particularly the lower bay, is quantified. Modifications of the various natural and artificial features on the flow field are examined.

Model Calibration and Verification

Results of a series of calibration runs indicate that Manning coefficients of 0.03 for the barren surface and 0.055 for seagrass beds produced the closest agreement between modeled and measured velocities. These values are greater than those (typically 0.025) used in other CMS-Flow modeling studies in this area (Beck *et al.*, 2020; Wang and Beck, 2012), reflecting the influence of shallow water and seagrass beds. Overall, the computed velocities compared well with the measured velocities at both bridges (Figure 4), with $S_w = 0.969$ at Bridge 1 and $S_w = 0.958$ at Bridge 2 (Equation [1]). These friction coefficients are used throughout this modeling study.

The calibrated model was verified by running the model over an approximately 6.5-day period after the calibration period. Overall, the computed velocities matched the measured values well at both bridges. The Willmott (1981) skill (Equation [1]) for the verification runs was similar to the calibration runs with $S_w = 0.972$ at Bridge 1, which is slightly lower than the $S_w = 0.978$ at Bridge 2. The high model skill values indicate that the Fort DeSoto Bay model constructed by this study provides accurate velocity computation.

Qualitative model verification was conducted based on observations during field data collection. Targeted field observations were conducted during the installation and periodic maintenance of the tide gauges and current meters, with a main goal of identifying areas in the lower bay with strong tidal driven flow other than at the two bridges. No areas with apparent strong flow were identified through field observations. This aligns with the numerical modeling results and is used here as a qualitative verification of the model.

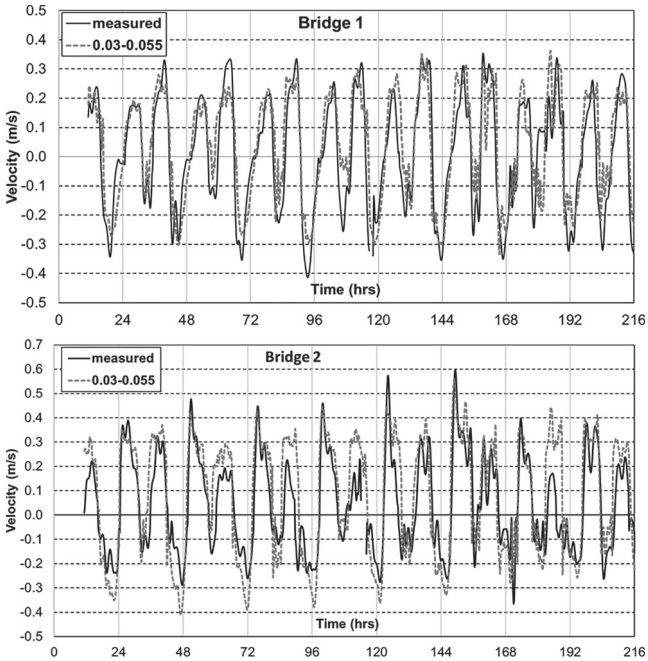

Figure 4. Measured and calculated velocities (with $n = 0.03$ for barren surface and $n = 0.055$ for seagrass beds) at both bridges. Zero hour on the horizontal axis is set at 10 August 2019 at 1615 hours.

Contribution of the Bridges to Water Exchange

Bridges and culverts are common methods for improving or restoring tidal circulation blocked by causeways in shallow estuaries. As shown in Figure 4, measured, as well as computed, peak tidal flows through both bridges can reach slightly over 0.5 m/s, which is by far the strongest flow in the lower Fort DeSoto Bay. It is worth emphasizing that both bridges are located near the southern terminus of the bay (Figure 3). This rather strong flow should contribute significantly to water mixing at the terminus of the bay. Improved water exchange is attributed as a major factor contributing to successful seagrass recovery in Tampa Bay (Sherwood *et al.*, 2017).

The contribution of the bridges to water exchange within Fort DeSoto Bay can be quantified from a water budget approach, *i.e.* comparing the discharges through the openings to the tidal prism of the bay. In addition to analyzing the entire bay, tidal exchange within the lower half of the bay, as defined in Figure 1, was also examined. Table 2 lists the computed discharges through the two bridges and the percentages relative to the tidal prism of the bay. Water exchange in the lower bay is significantly influenced by the two bridges, with nearly 26% of the tidal prism passing through the two bridges

Table 2. *Comparison of discharge through the two bridge openings with the tidal prism of Fort DeSoto Bay and the lower bay during a spring tide.*

	Both Bridges Open		Bridge 1 Blocked		Bridge 2 Blocked	
Flood discharge (m^3)	Q_{B1}	69,700	Q_{B2}	189,800	Q_{B1}	48,700
	Q_{B2}	218,700				
	$Q_{B1}+Q_{B2}$	288,400				
Ebb discharge (m^3)	Q_{B1}	69,700	Q_{B2}	115,500	Q_{B1}	53,000
	Q_{B2}	131,100				
	$Q_{B1}+Q_{B2}$	200,800				
% of flood prism: lower bay	Q_{B1}	6.21	Q_{B2}	16.91	Q_{B1}	4.34
	Q_{B2}	19.48				
	$Q_{B1}+Q_{B2}$	25.69				
% of ebb prism: lower bay	Q_{B1}	4.25	Q_{B2}	7.04	Q_{B1}	3.23
	Q_{B2}	7.99				
	$Q_{B1}+Q_{B2}$	12.24				
% of flood prism: entire bay	Q_{B1}	2.30	Q_{B2}	6.25	Q_{B1}	1.60
	Q_{B2}	7.20				
	$Q_{B1}+Q_{B2}$	9.50				
% of ebb prism: entire bay	Q_{B1}	1.57	Q_{B2}	2.60	Q_{B1}	1.19
	Q_{B2}	2.95				
	$Q_{B1}+Q_{B2}$	4.52				

during a spring flooding tide. It is worth noting that the 26% was obtained by summing the discharges through Bridges 1 and 2 (Table 2). It is possible that a portion of the water can flow through both bridges. Therefore, the 26% should represent the maximum amount.

The percentage of tidal prism passing through Bridge 2 is considerably larger than that through Bridge 1, particularly during flooding tide, 19.5% *vs*. 6.2% (Table 2), when water is flowing from west to east. This suggests that Bridge 2 has a larger area of influence than Bridge 1. This larger discharge can be explained by the fact that Bridge 2 receives water input from two sources (Figure 3): water flowing continually eastward from Bridge 1 and water flowing southward between the two causeways.

During ebbing tides, discharge is also greater at Bridge 2 than at Bridge 1 (Table 2), when water tends to flow from east to west. After passing through Bridge 2, a percentage of water exits the estuary northward between the two roughly parallel causeways, as opposed to flowing continually westward through Bridge 1. A greater percentage of tidal prism flows through the bridges during flood tides than during ebb tides, 26.0% *vs*.12.2%, for the two spring tides analyzed here (Table 2). This suggests that flooding currents tend to flow in a west-east direction and pass through the bridges, whereas ebbing currents tend to flow south-north and result in less discharge through the bridges as compared with flooding tides.

The numerical model also allows for examination of the influence of individual bridges to the water exchange and their interaction. This was conducted by artificially closing either Bridge 1 or Bridge 2 during the model simulations (*i.e*. Scenarios A4 and H6 in Table 1). As shown in Table 2, the discharge through one bridge decreases considerably when the other is closed, suggesting a strong hydrologic connection between the two bridges. Discharge during a flooding tide through Bridge 2 decreased from 19.5% of the lower bay prism when both bridges were open to 16.9% when Bridge 1 was closed, whereas for the ebbing tide, the discharge decreased from 8.0% to 7.0%. This represents a reduced water volume exchange of approximately 13% through Bridge 2 when Bridge 1 is closed. At Bridge 1, discharge during the studied flooding tide decreased from 6.2% of the lower bay prism when both bridges were open to 4.3% when Bridge 2 was closed, whereas for the ebbing tide, the discharge decreased from 4.3% to 3.2%. This represents a reduced water volume exchange of approximately 31% for flooding tide and 26% for ebbing tide through Bridge 1 when Bridge 2 is closed. This indicates that Bridge 2 has a relatively greater influence on Bridge 1 in terms of water exchange volume. This finding is somewhat unexpected given that Bridge 1 is located in the middle of the Bay and was opened first in 2004, as opposed to the 2016 opening of Bridge 2. This illustrates the value of numerical modeling in quantifying complicated tidal circulation in the terminus of a shallow estuary.

Modeled Flow Field under Different Scenarios

Ten scenarios were simulated, representing existing conditions, conditions before installation of the bridges, predevelopment natural conditions, and six hypothetical situations designed to examine various natural and anthropogenic factors (Table 1). Selected cases are presented to emphasize the influence of individual features such as causeways, dredged channels, and bridges.

Scenario A2: Existing Conditions with Both Bridges

Scenario A2 represents the existing conditions since 2016 after both bridges were constructed. This highly altered case is discussed here first because it is based on the most accurate data in terms of bathymetry, input tidal water-level variations, and verification with measured flow velocities. The results from the remaining scenarios were compared with this case.

Ebbing tide exits the bay flowing northward into Bunces Pass, while flooding tide enters the bay flowing southward (Figure 5). The dredged channels in the upper bay serve as efficient conduits for tidal exchange, with considerably stronger flow as compared to the surrounding shallow seagrass areas, although water exchange occurs along the entire north boundary. The flow in the upper bay is dominantly in the north-south direction, as confined by the causeways, mangrove islands, and the dredge channels.

The bridges provide conduits for east-west tidal currents, which flow parallel to the shoreline along the south bank

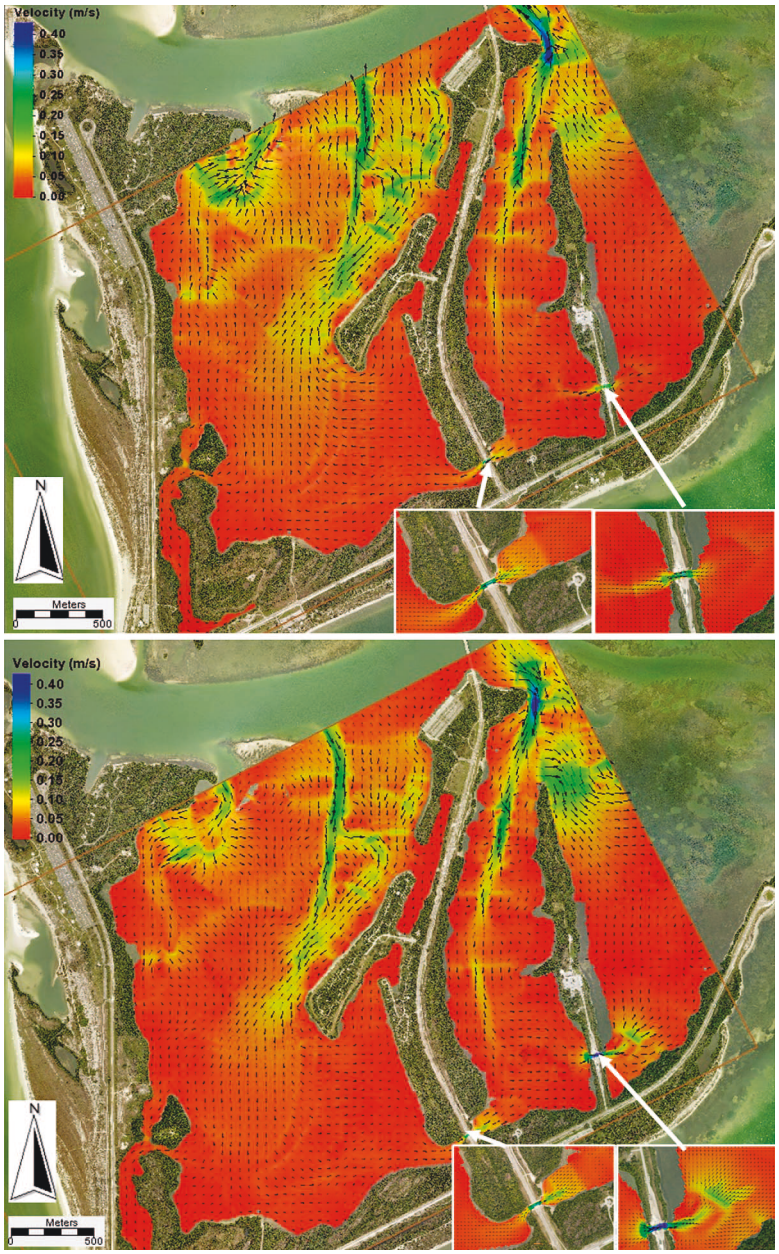

Figure 5. Modeled flow field under Scenario A2: existing conditions with both bridges. Upper panel: flow field under a peak ebb flow condition; lower panel: flow field under a peak flood flow condition. Insets at the bottom of each panel: closeup views of the flow fields at the two bridges.

(Figure 5). During the ebbing tide, the current flows from east to west through the two bridges and eventually exits the bay at Bunces Pass (Figure 5, upper panel). During the flooding tide, the current flows from west to east through both bridges (Figure 5, lower panel). This east-west flow also leads to a modest increase in the north-south flow in the dredged channels in the middle part of the bay, as compared with the pre-2004 A1 scenario without any bridges (Figure 6). The flow increase is more significant during peak flooding tide (Figure 6, lower panel) than during peak ebbing tide (Figure 6, upper panel). The increased north-south current likely feeds the east-west flow along the bottom of the bay. Therefore, the two bridges not only increased the tidal flow velocities in the stagnant southern terminus of the bay, but they also lead to a modest flow velocity increase in the dredged channels in the middle bay. The A2 existing condition serves as a main baseline case for comparison.

Case A3: Predevelopment Hydrodynamics

Scenario A3 represents the natural condition prior to the significant anthropogenic alterations. Comparing a recent

Figure 6. Flow difference map: both bridges closed minus existing conditions (A1–A2), positive value indicates stronger flow under the A1 condition, negative indicates weaker flow. Upper panel: under a peak ebb flow condition; lower panel: under a peak flood flow condition.

2020 aerial photo with a predevelopment one taken in 1943 (Figures 1 and 2), the human alterations that are directly relevant to tidal circulation include the two causeways connecting the mangrove islands and the south shore, dredged channels that are largely parallel to the causeways to provide the construction material, and two bridges near the south shoreline. These engineering alterations are rather common for shallow estuaries.

The bathymetry before human development is not known. The bathymetry used in the A3 model run was estimated based on the existing bathymetry, assuming that water depth over seagrass beds remains similar. A uniform depth of 0.6 m relative to mean tide level was used. The water depths in the gaps between the mangrove islands were estimated to be 1 m. Some uncertainties may arise from the estimated water depth. Specifically, the computed depth-averaged velocity magnitude through the gaps is influenced by the depth; however, the computed overall flow pattern should be adequate for the purpose of comparing with the altered conditions, *e.g.*, A2.

The tidal flow pattern in the upper bay under natural conditions (Figure 7) was quite different from that under existing conditions, largely attributable to the absence of the dredged channels (Figure 7). Without flow being concentrated within the dredged channels, the tidal current over the broad

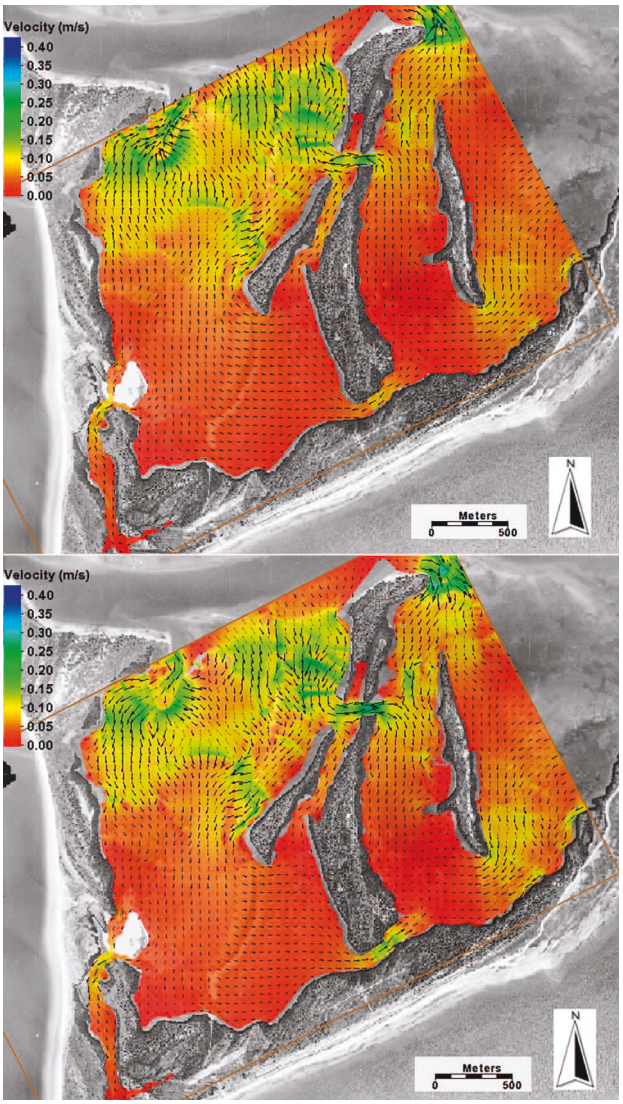

Figure 7. Modeled flow field under Scenario A3: predevelopment natural conditions. Upper panel: flow field under a peak ebb flow condition; lower panel: flow field under a peak flood flow condition. See Figures 1 and 2 for the names of various features.

shallow area south of Bunces Pass was much faster and more spatially uniform as compared to the existing A2 scenario (Figure 5) for both ebb and flood conditions. Strong east-west directed flow occurs through the gap in the middle of the bay, referred to here as Campground Pass. This east-west flow through the gap in the upper-middle bay may effectively isolate, to a certain extent, the middle and lower parts of the bay from water exchange via Bunces Pass to the north (Figure 7). This results in weaker tidal currents in the middle bay as compared with the existing A2 conditions (Figures 5 and 7).

The two wide gaps between the south shoreline and the two large mangrove islands (Figure 2, MI1 and MI2) facilitated the tidal flow in the lower bay (Figure 7). However, a significant amount of the water flowing through the wide gap to the east originates from the east boundary, particularly the southern portion of the boundary. The flow through the narrower gap to the west appears to come mostly from the north boundary, Bunces Pass. This results in opposite flow directions at the two gaps (Figure 7). Under peak ebb flow conditions (Figure 7, upper panel), the flow through the gap to the west is directed to the west, eventually exiting the bay at Bunces Pass. The flow through the wide gap to the east is directed to the east and exits the lower bay at the southeast boundary (Figure 7, upper panel). This results in a diverging zone in the middle of the bay between the two large mangrove islands (Figure 2, MI1 and MI2). Under peak flood flow conditions (Figure 7, lower panel), the flow through the gap to the west is directed to the east, indicating its origin from Bunces Pass. The flow through the wide gap to the east is directed to the west, suggesting that the water originates from the east boundary (Figure 7, lower panel). This results in a converging zone in the middle of the bay between the two large mangrove islands.

Under the existing conditions with the dredged channels extending to the south end of the bay, the tidal flows through the two bridges are in the same direction under both flooding and ebbing tides with water coming in and exiting mostly from Bunces Pass (Figure 5). This is opposite to the diverging or converging flow under the natural shallow conditions (Figure 7) with significant water exchange occurring at both north and east boundaries. This suggests that the dredged channels have greatly improved the efficiency of water exchange with Bunces Pass. In addition, the dredged channels have fundamentally changed the tidal flow patterns, both in magnitude and direction, in the lower bay.

Scenarios H4 and H3: Filling the Dredged Channels and the Large Dredged Hole

The H4 scenario examines the option of filling the dredged channels and restoring the bathymetry in Fort DeSoto Bay to its predevelopment conditions while maintaining the causeways and the two bridges. This case isolates and examines the influence of dredged channels on the tidal circulation pattern. To more directly compare with A2 and A3 cases described previously, H4 is discussed here first before other hypothetical cases.

In the upper bay, the H4 flow pattern (Figure 8) more resembles the predevelopment natural A3 conditions (Figure 7) than the existing A2 conditions (Figure 5), confirming the significant control of the dredged channels. The H4 tidal flow distributes rather homogenously over a large area without significant channelization. Different from the predevelopment natural conditions, no east-west flow occurs because of the closure of Campground Pass (Figures 1 and 2).

In the lower bay, the flow magnitudes through both bridges appear to be slightly stronger as compared with the existing A2 conditions under the peak ebbing and flooding conditions (Figures 8 and 5). Also similar to the case of predevelopment natural conditions and opposite to the existing A2 conditions, the flows through the two bridges are directed in opposite directions, with flow through the east bridge (Bridge 2) controlled by the nearby east boundary and flow through the west bridge (Bridge 1) being controlled by Bunces Pass to the north. Without the dredged channels serving as efficient

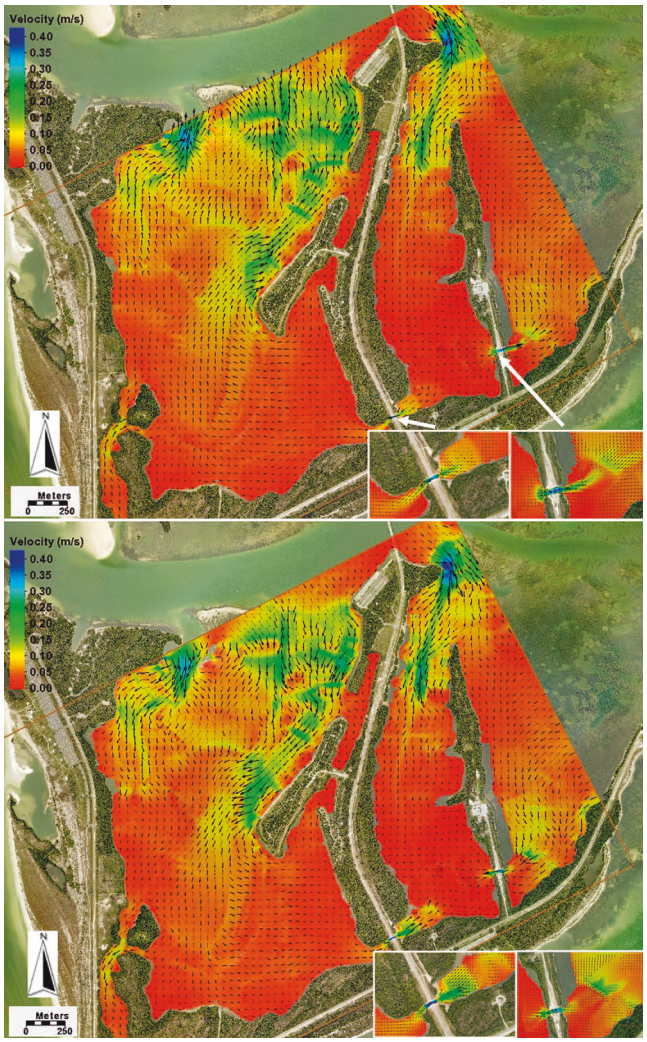

Figure 8. Modeled flow field under Scenario H4: filling of dredged channels. Upper panel: flow field under a peak ebb flow condition; lower panel: flow field under a peak flood flow condition. Insets at the bottom of each panel: closeup views of the flow fields at the two bridges.

conduits for water exchange with Bunces Pass, the water exchange at Bridge 2 is dominated by the east boundary, particularly the southern stretch.

In the middle bay (in the vicinity of the dividing line in Figure 1), also similar to the natural A3 case, a diverging and converging zone occurs between the two causeways during ebbing and flooding tides, respectively. This results in a rather stagnant area with very weak flow (Figure 8). Therefore, the H4 scenario confirms that the dredged channels improved the tidal flow velocity in the middle bay by allowing water exchange with Bunces Pass to be more efficient. Overall, the flow pattern changes caused by filling the dredged channels suggest that the dredged channels are the most significant anthropogenic factor influencing the tidal circulation in Fort DeSoto Bay.

The large (~21.5 acres, 87,000 m^2), isolated dredged hole in the SW corner of Fort DeSoto Bay (Figure 3) was excavated to nearly 4.4 m to provide material for causeway construction. This area had low-flow velocity before the dredging. The much deeper water after the dredging led to even weaker flow. The stagnant water in this man-made deep hole resulted in poor water quality, stratification, and sediment toxicity (Raulerson *et al.*, 2019). As a mitigation measure, it was proposed that the dredged hole be filled with 88,000 m^3 of sediment to its surrounding roughly 1 m water depth (Raulerson *et al.*, 2019). Filling the hole to surrounding water depth has negligible influence on the tidal circulation pattern in the entire Fort DeSoto Bay, as well as in the lower bay and in the vicinity of the hole.

Scenario H1: Bridges Closed and Dredged Channels Filled

This scenario removes all the channel features within Fort DeSoto Bay while leaving the emerged features, such as causeways and islands, in place. The dredged channels were filled to the surrounding depth. The east-west–directed tidal flows are completely blocked by the causeways in the absence of the bridges. This hypothetical case is similar to the A1 case, *i.e.* the actual condition before 2004, except with the dredged channels filled. It is different from the predevelopment conditions in that all the natural gaps that facilitate east-west tidal flow are blocked.

The H1 case has relatively strong flow over a large area in the upper bay (Figure 9). Without the efficient north-south–dredged channels, the flow is mostly limited to the upper bay with less penetration to the lower bay. This hypothetical scenario results in the most stagnant water in the lower bay (Figure 9) among all the 10 cases (Table 1). The rather uniform flow pattern in the upper bay bares considerable similarity with the A3 predevelopment natural conditions (Figure 7), both without the dredged channels. However, with the east-west flow through the Campground Pass blocked, the north-south–directed flow is stronger in the H1 case than in the A3 case; and extends slightly further into the middle bay to just south of the divide (Figure 1).

DISCUSSION

The circulation patterns in Fort DeSoto Bay are influenced by various natural and artificial features including natural channels, mangrove islands, seagrass beds, causeways, dredged channels, and bridges. These features are not unique to Fort DeSoto Bay and are common in shallow estuaries. Connecting existing emerged landforms and using material dredged along the roadway can be an economic way of constructing causeways, and therefore has been historically applied. This was the case at Fort DeSoto Bay. Because causeways obstruct tidal flow, bridges are often installed at strategic locations to facilitate water exchange. Well-established numerical models provide valuable tools to investigate various factors influencing tidal circulation in estuaries.

Influence of Causeways on Circulation

Causeways act as physical barriers that obstruct the tidal flow moving in a perpendicular direction. Therefore, if the causeway-perpendicular flow is essential to the circulation, as

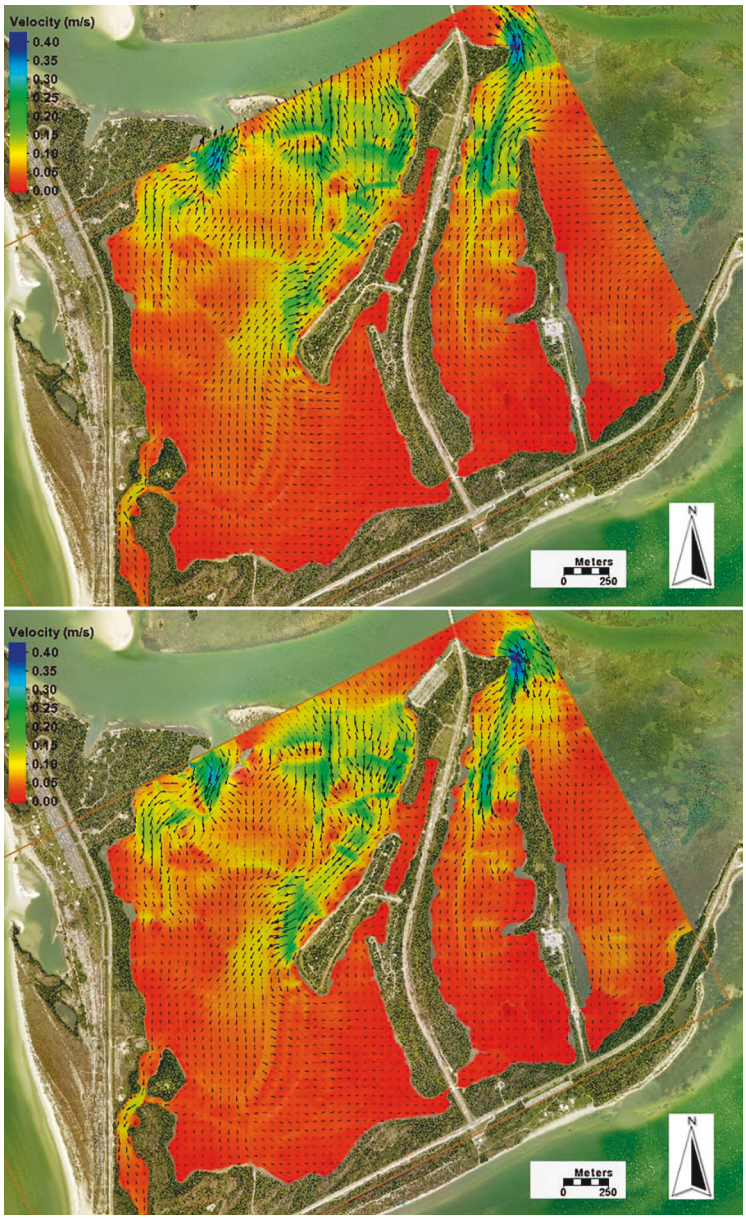

Figure 9. Modeled flow field under Scenario H1: with bridges closed and dredged channels filled. Upper panel: flow field under a peak ebb flow condition; lower panel: flow field under a peak flood flow condition.

is the case with Fort DeSoto Bay, the effects can be quite negative. The construction of the two north-south–oriented causeways in Fort DeSoto Bay compartmentalized the estuary into three cells and eliminated east-west tidal flow, which was a critical component of the natural circulation patterns. This led to a reduction in flow velocities and subsequently water quality particularly in the lower bay. These effects were highlighted in Case A1 showing that unbroken causeways lead to nearly stagnant flow conditions in the middle and lower bay. The stagnant water diminishes the habitat quality of seagrass beds (Sherwood *et al*., 2017). Figure 10 illustrates the computed flow velocities at 11 locations throughout Fort DeSoto Bay for the A1 scenario with east-west flow completely blocked by the causeways. The tidal-driven flow velocities in the lower bay rarely exceed 0.02 m/s.

The conditions presented here are not unique to Fort DeSoto Bay. Florida's Gulf and Atlantic coasts are fringed with barrier islands that are connected to the mainland with causeways. Many of these causeways extend perpendicular to the flow direction and cross important estuarine habitats such as seagrass beds, salt marsh, and mangrove islands, which rely on regular tidal flow to mediate physiochemical and biological

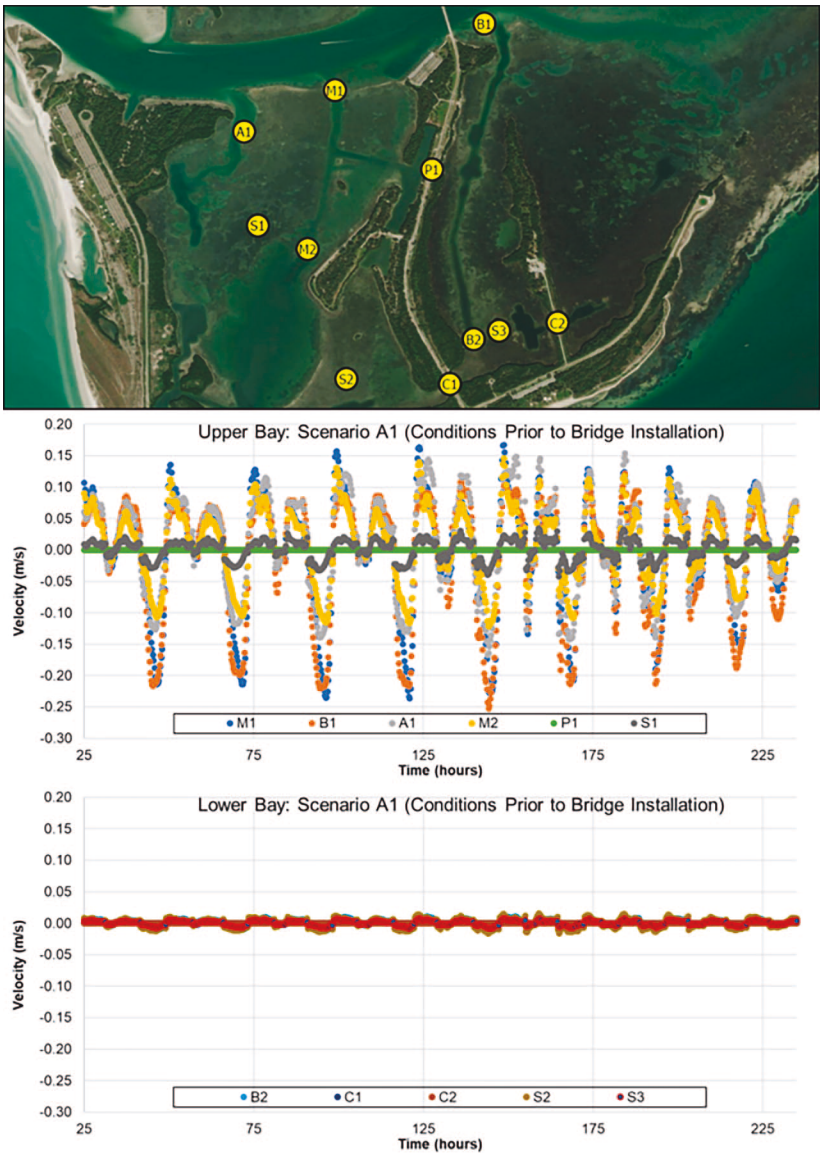

Figure 10. Tidal flow at 11 points of interest for case A1 (no bridges). Upper panel: locations of the numerical flow stations; middle panel: flow in the upper bay; lower panel: flow in the lower bay. Positive velocity represents flood flow; negative velocity represents ebb flow.

processes. The practice of constructing causeways over shallow habitats or by connecting mangrove islands is less costly and was therefore historically applied. For example, the construction of the Sanibel Island causeway blocked connectivity between Clam and Dinkins Bayous, which led to the loss of 120 acres of seagrass beds, elimination of scallop populations, and frequent algal blooms and fish kills in lower Pine Island Sound, SW Florida (Craig *et al.,* 2010). The construction of three box culverts in strategic locations along the causeway reestablished natural tidal flushing and salinity levels (Craig *et al.,* 2010). These case studies provide important evidence to show decision makers that even minor restoration projects, box culverts in this case, can significantly improve estuarine habitat quality. An adequate understanding of tidal circulation patterns through numerical modeling is essential for guiding restoration projects.

Contribution of Bridges to Water Exchange and Seagrass Recovery

The two 12-m-span bridges in the southern part of Fort DeSoto Bay were installed with the goal of restoring historical tidal circulation patterns, improving water quality, and restoring seagrasses. The contribution of these bridges to hydrodynamic exchange can be inferred by the postconstruction habitat monitoring data, which showed reduced physiochemical stress over a 3-year period following construction of Bridge 1 (Craig *et al*., 2010), as well as a recovery of approximately 200 acres of seagrass (*T. testudinum*) in areas

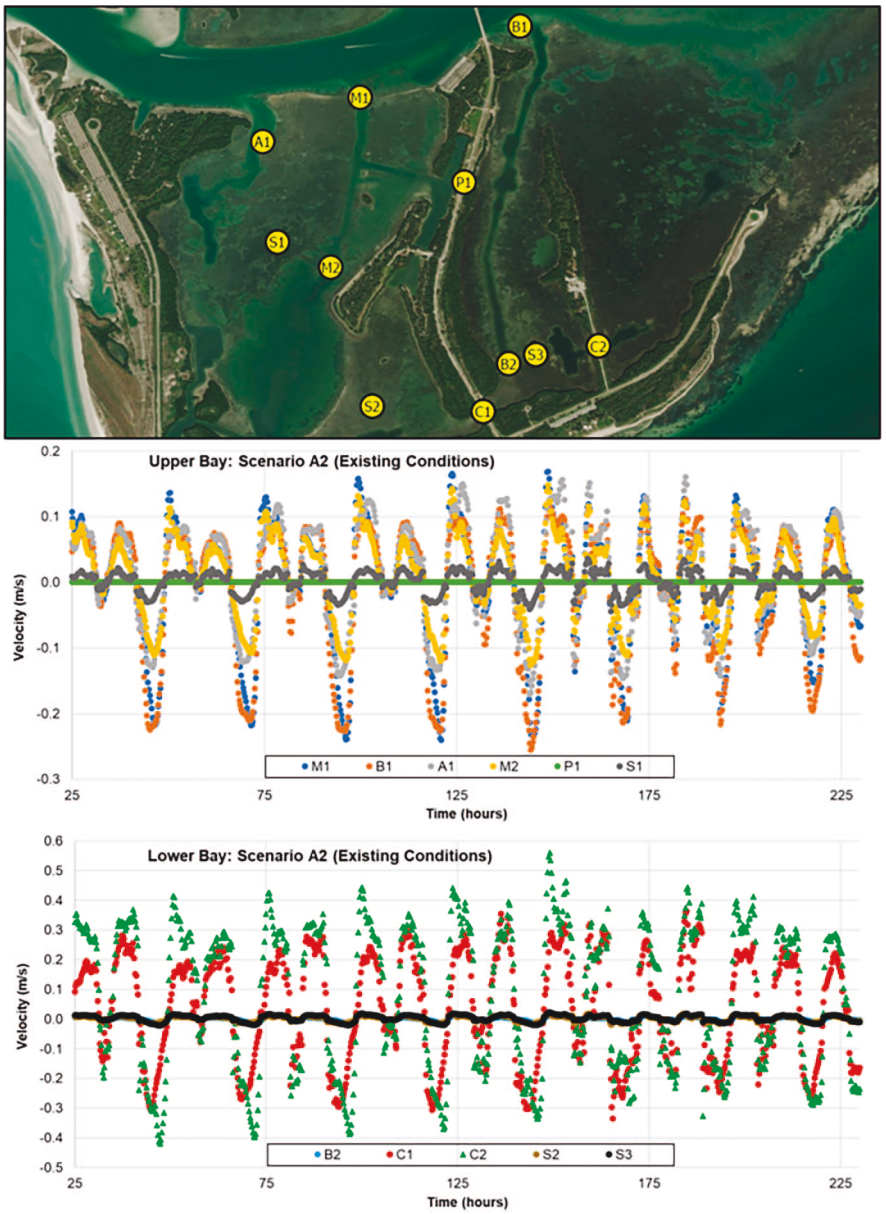

Figure 11. Tidal flow at 11 points of interest for case A2 (both bridges). Upper panel: locations of the numerical flow stations; middle panel: flow in the upper bay; lower panel: flow in the lower bay. Positive velocity represents flood flow; negative velocity represents ebb flow.

that were previously barren (Tampa Bay Estuary Program, 2017). Numerical modeling confirms the contribution of the bridges to improved water exchange. Prior to bridge installation (Scenario A1), current velocities were lower than 0.02 m/s within most of the lower bay (Figure 10). This reduced flow is likely what contributed to temperature loading, low dissolved oxygen, and seagrass mortality in the southern bay (Tampa Bay Estuary Program, 2017). Bridge construction resulted in significant increases in tidal flow velocities in the lower bay (Figure 11). Measured, as well as computed, peak tidal flows through both bridge openings can reach 0.5 m/s, which is by far the strongest flow in the lower Fort DeSoto Bay. The combined discharge at the bridges represents up to 25% of the tidal prism of the lower bay (Table 2).

In addition to quantifying the effects of the bridge openings, the modeling results provide insights into the complicated tidal circulation patterns in the terminus of a shallow estuary. For example, both the tidal prism analysis and computed flow field suggested a larger water discharge and area of influence for Bridge 2 than for Bridge 1. This can be explained by the fact that Bridge 2 receives hydrologic input from two sources during flooding: water flowing continuously eastward from Bridge 1 and water flowing southward between the two causeways. Discharge is also greater at Bridge 2 during the ebb tide, when

water flows from east to west. A portion of the water flowing westward through Bridge 2 exits the estuary between the parallel causeways, as opposed to continually flowing through Bridge 1. The larger area of influence and discharge through Bridge 2 is somewhat unexpected given that Bridge 1 is more centrally located in the Bay and was constructed 12 years prior to Bridge 2.

The Fort DeSoto Bay bridge project did not remove sections of the causeway at a historical tidal conduit in the northern portion of the bay, *i.e*. the closed Campground Pass (Figures 1 and 2). The Campground Pass was filled in when the causeway was constructed and remains closed to this day. Scenario H2 (Table 1) examined the case of installing a circulation bridge at this location. Given its location further north in the bay where circulation is relatively active due to proximity to Bunces Pass, closing of this conduit had a negligible influence on water quality and ecosystem health in the upper bay. However, the east-west flow in the upper bay reduced the strength of north-south flow toward the southern lower bay. The numerical model yielded a considerably reduced flow velocity through Bridge 1 and an overall reduction in the middle and lower bay. Therefore, while reopening this historic tidal conduit would restore the Fort DeSoto Bay closer to its predevelopment conditions, the increased tidal flow velocity in the upper bay comes at the expense of reduced circulation in the stagnant middle and lower bay.

In summary, numerical models can help evaluate various circulation improvement alternatives using bridges. For the case of Fort DeSoto Bay, despite its central location, Bridge 1 offers a smaller area of influence and water discharge as compared to Bridge 2. From a management point of view, opening of Bridge 2 should have higher priority than Bridge 1. Restoring the Campground Pass in the upper bay may bring the system closer to its natural conditions. However, this would diminish the quality of the already stagnant middle and lower bay. The numerical modeling of hypothetical scenarios provided insights on optimizing circulation efficiency at the terminus of shallow estuaries.

Influence of Dredged Channels and Seagrass Beds on Circulation

Natural and dredged channels have significant influence on circulation patterns in shallow estuaries by providing efficient conduits for tidal flow. For the case of Fort DeSoto Bay, the channels were not dredged for navigation or circulation purposes. Instead, they were dredged largely parallel to the causeways to provide material for their construction. The narrow and linear geometry of the north-south–extending dredged channels concentrate tidal flow entering and existing the estuary from and to Bunces Pass. The increased flow within the dredged channels is compensated by an overall decreased flow velocity over the broad adjacent seagrass beds. These findings are consistent with those of Weisberg and Zheng (2006) and Galperin, Blumberg, and Weisberg (1992), who found that an internal pressure gradient drives currents into the Tampa Bay through deeper dredged channels, leading to greater in-channel velocities. DelCharco (1998) found through field measurements that the dredged Intracoastal Waterway played a significant role in influencing circulation patterns in the shallow Pine Island Sound, a subestuary in Charlotte Harbor, SW Florida. Similarly, Wang, Beck, and Roberts (2011) found through numerical modeling that the dredged Intracoastal Waterway played a significant role in tidal flow patterns in Boca Ciega Bay, west-central Florida and suggested that accurately representing the often-narrow waterway was essential to simulating the flow field. In contrast, if the dredged channel is wide and deep, it may still concentrate the flow but with lower velocity as compared with the predredging case due to the increased cross-sectional area (Martelo *et al*., 2019).

For the case of Fort DeSoto Bay, the dredged channels not only influence the tidal flow velocities but also the overall flow pattern. This is illustrated by comparing the circulation pattern under existing conditions A2 with dredged channels to that under predevelopment conditions A3 without the channels (Figures 5 and 7). Under the no-channel conditions, flood-tidal currents followed a west to east direction through the west gap (where Bridge 1 was installed) and an east to west direction through the east gap (Bridge 2 location). This leads to a flow convergence zone between the two large mangrove islands during flooding tide and a divergent zone during ebbing tide. These converging and diverging flow patterns were not computed nor measured under the existing A2 conditions with the dredged channels (Figure 5).

Analysis of the film loop of the computed flow field reveals that the dredged channels are the dominant cause of the altered circulation pattern. A conceptual model was developed and illustrated in Figure 12. The predevelopment conditions, as depicted from a 1943 aerial photo (Figure 2), differs from the present artificially altered conditions in that no north-south–oriented dredged channels occurred; two wide and shallow gaps occurred at the bottom of the bay, where the bridges are; and a gap occurred between the two large mangrove islands in the upper middle bay. Without the dredge channels concentrating currents, the flood current flow southward over the seagrass beds in the upper bay is spatially uniform, reaching about 0.15 m/s. The strongest flow in the upper bay occurs in the east-west–oriented Campground Pass, reaching 0.25 m/s flowing eastward. In the lower bay, flow through the wide gaps near the southern shoreline reaches 0.15 m/s. Without the dredged channels acting as conduits, the flow velocity in the middle bay tends to be low. A considerable amount of water exchange in the lower bay originates from the SE boundary with the greater Tampa Bay (Figure 1). This leads to a significant difference in flow patterns between the predevelopment conditions and existing conditions (Figure 12). For the ebbing tide, the flow follows a similar pattern but in opposite directions as shown in Figure 12. The main cause of this difference in flow patterns between predevelopment and altered conditions is the dredged channels, which allow the water to reach the lower bay more efficiently than the cases without them.

The hydrodynamic response, as described previously, was likely not considered in the initial channel dredging design. Bunces Pass to the north serves as the main tidal connection to the sea, and the north-south–oriented channels allow for further and more rapid penetration of tidal currents to the lower bay during the flood tide and more efficient flushing during the ebb tide. It is therefore reasonable to conclude that

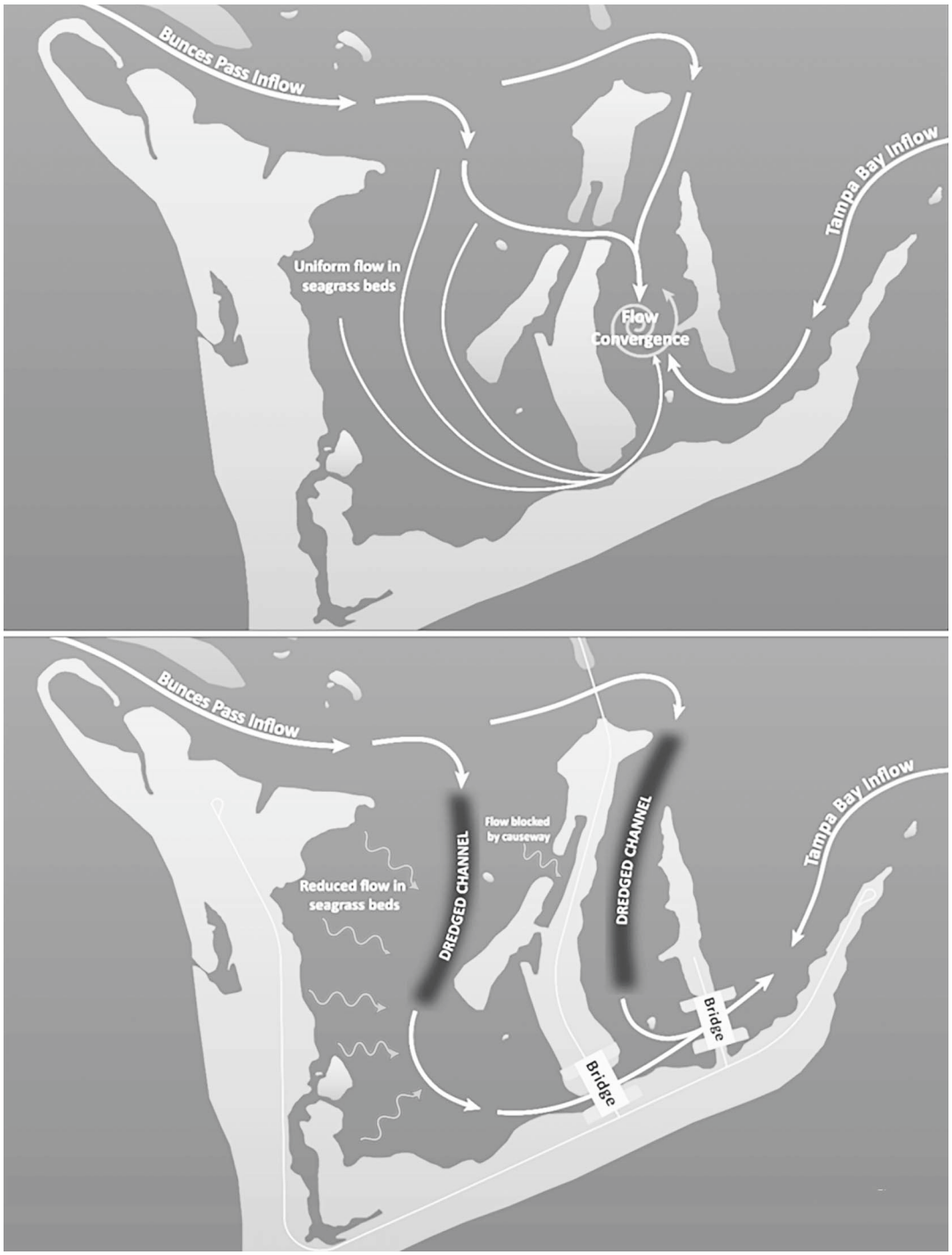

Figure 12. A conceptual model depicting generalized tidal flow pattern in Fort DeSoto Bay during a flooding tide. Upper panel: under predevelopment natural conditions; lower panel: under existing conditions. Ebb flow follows similar pattern but in the opposite direction.

the dredged channels reduced the residence time of water and aided in hydrologic flushing of detritus and contaminants from the terminus of the bay. These results are consistent with the findings of Linville (2007), which demonstrated that dredged channels resulted in stronger flow and reduced flushing time. Van Maren (2015) similarly found that channel deepening increased estuarine circulation and sediment transport.

The previous results suggest that dredged channels can be designed to guide tidal water to stagnant portions of a bay. Specifically, dredged channels can be designed to guide the

tidal flow in a desirable direction and, therefore, alter the circulation patterns in a way that is beneficial to water quality and ecosystem health. The degree of flow alteration depends on the orientation of the channel with respect to the dominant flow direction. Channels parallel to the dominant flow directions, as is the case at Fort DeSoto Bay, are most efficient in directing water to the terminus of a bay. Large cross-sectional area may result in reduced flow velocity in the channel, whereas small cross-sectional area increases velocity. However, flow concentration in the dredged channels can come at the expense of reduced flow velocity in the adjacent shallow areas. Furthermore, dredging has been shown to adversely impact seagrasses through physical removal and/or burial of vegetation and increased water turbidity (Erftemeijer and Lewis, 2006). Therefore, the potential negative influence on the surrounding areas should be carefully considered when using dredged channels to improve tidal circulation in a certain part of a bay.

Natural vs. Altered Circulation Patterns and Considerations in Flow Restoration

The natural circulation patterns are generally considered as a desirable scenario that is often used to guide flow restoration strategies in estuaries. Prior to human interventions, Fort DeSoto Bay was characterized by a rather uniform bathymetry. The bay was segmented by mangrove islands (Figure 2). Gaps existed between the islands, allowing both north-south– and east-west–directed tidal circulation. However, zones of flow divergence and convergence exist in the lower middle bay, resulting in localized stagnation.

Although the natural circulation patterns are desirable, it can be argued that human-induced alterations are inevitable due to the desire to live along the estuarine shoreline. As illustrated by the case at Fort DeSoto Bay, historical human alteration is controlled by environmental regulations at the specific time. For example, the construction of the causeways and channel dredging in the 1950s and subsequent compartmentalization of the bay would not be allowed under present environmental regulations. From a different perspective, modern flow restoration projects are developed upon the existing altered conditions. For the case of Fort DeSoto Bay, circulation bridges were installed at strategic locations on the causeway. It may not be economically nor logistically feasible to reverse all of anthropogenic modifications that have taken place, *i.e*. removing the entire causeway and filling the dredge channels. Therefore, resource managers must decide whether to restore the natural environment that existed before anthropogenic modification or to create a different target ecosystem (Burger *et al*., 2007). In the case of Fort DeSoto Bay, the latter was the case, involving the installation of two bridges near the bottom of the bay where the natural gaps existed, while leaving the dredged channels in place. Compared to the natural condition A3 (Figure 7), the existing condition A2 (Figure 5) has improved circulation in the stagnant middle bay (Figure 12). Therefore, considerations for flow restoration should balance natural conditions and existing altered conditions.

Craig *et al*. (2010) developed a list of long-term indicators of ecological change that are intended to help identify areas within estuaries that could benefit from tidal restoration. These indicators include changing water quality, shifts in benthic assemblages, algal proliferation, vegetative die-offs, and invasions of non-native species. Optimizing the location of tidal bridges also requires an understanding of historical flow patterns and land mass boundaries, which can be obtained using historical imagery. Using environmental indicators in conjunction with hydrodynamic modeling provides a holistic approach to determining which restoration locations would provide the greatest mitigation potential. An in-depth understanding and ability to accurately compute the influences of various anthropogenic activities on circulation can help minimize prolonged impact on estuarine habitats and identify cost-effective and practicable solutions.

CONCLUSIONS

A calibrated and verified numerical model was developed to evaluate the influence of causeways, dredged channels, tidal bridges, mangrove islands, and seagrass beds on tidal circulation patterns at a shallow seagrass estuary, Fort DeSoto Bay. Causeways compartmentalized the shallow estuary and blocked east-west flow, which was partially restored by the installation of two bridges. The bridges significantly improved tidal exchange in the relatively stagnant southern terminus of the bay, with up to 26% of the flood tidal prism in the lower bay passing through the openings during a tidal cycle. In addition to mitigating the circulation blockage caused by the causeways, the bridges also increased flow velocities in the stagnant middle bay. The two bridges do not contribute equally to tidal circulation, with one bridge dominating over the other. A numerical model is valuable in quantifying the contributions of tidal bridges to circulation and therefore provides an important decision-making tool. Dense seagrass beds increase bottom friction and attenuate tidal flow. The dredged channels concentrate tidal flow entering and exiting the shallow estuary, leading to greater velocities within the channels and corresponding reduced velocities in the adjacent seagrass beds. The dredged channels play a central role in controlling tidal circulation within this shallow estuary. They not only changed the flow velocity, but also altered the spatial and temporal flow patterns. From a management point of view, channels can be designed to improve tidal circulation in stagnant portions of an estuary, aided by a well-established numerical model.

ACKNOWLEDGMENTS

This study was funded by Pinellas County, Florida. Graduate students Mathieu Valle, Jacob Adam, and Francesca Toledo assisted with field data collection. Special thanks to the Fort DeSoto Park staff for accommodating research crews during the installation and maintenance of field equipment.

LITERATURE CITED

Abdelrhman, M.A., 2003. Effect of eelgrass *Zostera marina* canopies on flow and transport. *Marine Ecology Progress Series*, 248, 67–83.

Beck, T.M. and Wang, P., 2019. Morphodynamics of barrier-inlet systems in the context of regional sediment management, with case studies from west-central Florida, USA. *Ocean and Coastal Management*, 177, 31–51.

Beck, T.M.; Wang, P.; Li, H., and Wu, W., 2020. Sediment bypassing pathways between tidal inlets and adjacent beaches. *Journal of Coastal Research*, 36(5), 897–914.

Brockmeyer, R.E.; Rey, J.R.; Virnstein, R.W.; Gilmore, R.G., and Earnest, L., 1997. Rehabilitation of impounded estuarine wetlands by hydrologic reconnection to the Indian River Lagoon, Florida. Special Issue: Hydrologic Restoration of Coastal Wetlands. *Wetlands Ecology and Management*, 4, 93–109.

Bryan, K.R.; Tay, H.W.; Pilditch, C.A.; Lundquist, C.J., and Hunt, H.L., 2007. The effects of seagrass (*Zostera muelleri*) on boundary-layer hydrodynamics in Whangapoua Estuary, New Zealand. *In:* Lemckert, C.J. (ed.), *Proceedings from the International Coastal Symposium (ICS)*. *Journal of Coastal Research*, Special Issue No. 50, 668–672.

Burger, J.; Gochfeld, M.; Powers, C.W., and Greenberg, M., 2007. Defining an ecological baseline for restoration and natural resource damage assessment of contaminated sites: The case of the Department of Energy. *Journal of Environmental Planning and Management*, 50(4), 553–566.

Craig, L.; McCraken, K.; Schnabolk, H., and Ward, B., 2010. *Returning the Tide: A Tidal Hydrology Restoration Guidance Manual for the Southeastern United States*. Silver Spring, Maryland: NOAA, 213p.

DelCharco, M.J., 1998. *Tidal Flow in Selected Areas of Tampa Bay* and Charlotte Harbor, *Florida, 1995–96*. U.S. Tallahassee, Florida: Geological Survey*, Water-Resources Investigations Report 97-4265*, 48p.

Dyer, K.R., 1997. *Estuaries, A Physical Introduction*, 2nd edition. New York: Wiley, 210p.

El Allaoui, N.; Serra, T.; Colomer, J.; Soler, M.; Casamitjana, X., and Oldham, C., 2016. Interactions between fragmented seagrass canopies and the local hydrodynamics. *PloS One*, 11(5), e0156264.

Erftemeijer, P.L.A. and Lewis III, R.R.R., 2006. Environmental impacts of dredging on seagrasses: A review. *Marine Pollution Bulletin*, 52, 1553–1572.

Fang, S.; Xie, Y., and Cui, L., 2015. Analysis of tidal prism evolution and characteristics of the Lingdingyang Bay at Pearl River Estuary. *MATEC Web of Conferences*, 25, 10.

Flindt, M.R.; Pardal, M.A.; Lillebo, A.I.; Martins, I., and Marques, J.C., 1999. Nutrient cycling and plant dynamics in estuaries: A brief review. *Acta Oecologica*, 20, 237–248.

Fonseca, M.S. and Fisher, J.S., 1986. A comparison of canopy friction and sediment movement between four species of seagrass with reference to their ecology and restoration. *Marine Ecology Progress Series*, 29, 15–22.

Galperin, B.; Blumberg, A., and Weisberg. R., 1992. A time-dependent three-dimensional model of circulation in Tampa Bay. *In:* Zervas, C.E. (ed.), *Proceedings, Tampa Bay Area Scientific Information Symposium,* 2, pp. 77–98.

Goodwin, C.R., 1987. *Tidal-Flow, Circulation, and Flushing Changes Caused by Dredge and Fill in Tampa Bay, Florida*. Denver: U.S. Geological Survey*, Water-Supply Paper 2282*, 87p.

Hansen, J.C.R. and Reidenbach, M.A., 2012. Wave and tidally driven flows in eelgrass beds and their effect on sediment resuspension. *Marine Ecology Progress Series*, 448, 271–287.

Heck, K.I., Jr.; Nadeau, D.A., and Thomas, R., 1997. The nursery role of seagrass beds. *Gulf of Mexico Science*, 15(1), 50–54.

Le Bouteiller, C. and Venditti, J.G., 2015, Sediment transport and shear stress partitioning in a vegetated flow. *Water Resources Research*, 51, 2901–2922.

Le Bouteiller, C. and Venditti, J.G., 2014. Vegetation-driven morphodynamic adjustments of a sand bed. *Geophysical Research Letters*, 41, 3876–3883.

Linville, A.J., 2007. Bathymetric Alterations Due to Urbanization and Their Effects on Residual Salinity, Flow Field and Transport Time for Tampa Bay, Florida. Tampa, Florida: University of South Florida, Master's thesis, 98p.

Martelo, A.F.; Trombetto, T.B.; Lopes, B.V.; Marques, W.C., and Möller, O.O., 2019. Impacts of dredging on the hydromorphodynamics of the Patos Lagoon estuary, southern Brazil. *Ocean Engineering*, 188, 106325.

Moki, H.; Taguchi, K.; Nakagawa, Y.; Montani, S., and Kuwae, T., 2020. Spatial and seasonal impacts of submerged aquatic vegetation (sav) dragforce on hydrodynamics in shallow waters. *Journal of Marine Systems*, 209, 103373.

Paquier, A.-E.; Oudart, T.; Le Bouteiller, C.; Larroude, S.E.P., and Dalrymple, R.A., 2020. 3D numerical simulation of seagrass movement under waves and currents with GPUSPH. *International Journal of Sediment Research*, 36, 711–722.

Peterson, C.H.; Richard A.; Luettich Jr., R.A.; Micheli, F.A., and Skilleter, G.A., 2004. Attenuation of water flow inside seagrass canopies of differing structure. *Marine Ecology Progress Series*, 268, 81–92.

Pickering, D.; Jones, A.; Aldous, A., and Schindel, M., 2018. *Where Road Projects Could Improve Oregon's Estuaries and Benefit Local Communities*. Portland, Oregon*:* The Nature Conservancy, 17p.

Raulerson, G.E.; Hershorin, A.G.; Karlen, D.J.; MacDonald, T.C., and Tyler-Jedlund, A.J., 2019. *Tampa Bay Dredged Hole Assessment and Management Recommendations: 2019 Synthesis Report*. St. Petersburg, Florida: Tampa Bay Estuary Program, *TBEP Technical Report #2019-02,* 66p.

Rose, L.V., 2008. Effects of Habitat Fragmentation and Restoration on Fish Assemblage Structure and Function. Tuscaloosa, Alabama: University of Alabama, Ph.D. dissertation, 120p.

Sanchez, A.; Wu, W., and Beck, T.M., 2016. A depth-averaged 2-D model of flow and sediment transport in coastal waters. *Ocean Dynamics*, 66(11), 1475–1495.

Sanchez, A.; Wu, W.; Beck, T.M.; Li, H.; Rosati III, J.; Thomas, R.; Rosati, J.D.; Demirbilek, Z.; Brown, M., and Reed, C., 2011. *Verification and Validation of the Coastal Modeling System, Report 3: CMS-Flow: Hydrodynamics*. Vicksburg, Mississippi: U.S. Army Engineer Research and Development Center, Coastal and Hydraulics Laboratory, 148p.

Sanchez, A.; Wu, W.; Li, H.; Brown, M.; Reed, C.; Rosati, J.D., and Demirbilek, Z., 2014. *Coastal Modeling System: Mathematical Formulations and Numerical Methods*. Vicksburg, Mississippi: Army Engineer Research and Development Center, Coastal and Hydraulics Laboratory, 102p.

Sherwood, E.; Greening, H.; Johansson, J.O.; Kaufman, K., and Raulerson, G.E., 2017. Documenting seagrass recovery since the 1980s and reviewing the benefits. *Southeastern Geographer*, 57, 294–319.

Southwest Florida Water Management District (SWFWMD), 2018. *2018 Florida Department of Transportation (FDOT) Mitigation Plan*. Brooksville, Florida: SWFWMD, 336p.

Tampa Bay Estuary Program, 2017. *Environmental Compliance Document*. https://www.restorethegulf.gov/sites/default/files/EC_Tampa_Bay_NEP_Compliance_Documentation_Five_Actions_20170417.pdf

Terrados, J. and Borum, J., 2004. Why are seagrasses important? Goods services provided by seagrass meadows. *In:* Borum, J.; Duarte, C.M.; Krause-Jensen, D., and Greve, T.M. (eds.), *European Seagrasses: An Introduction to Monitoring and Management*, Copenhagen, Denmark: M&MS Project, pp. 8–10.

Tomasko, D.A., 2000. Status and trends of seagrass coverage in Tampa Bay, with reference to other Southwest Florida estuaries. *In:* Greening, H.S. (ed.), *Seagrass management, It's not just nutrients!* St. Petersburg, Florida: Tampa Bay Estuary Program, pp. 11–20.

Van Katwijk, M.M.; Thorhaug, A.; Marbà, N.; Orth, R.J.; Duarte, C.M.; Kendrick, G.A.; Althuizen, I.H.J.; Balestri, E.; Bernard, G.; Cambridge, M.L.; Cunha, A.; Durance, C.; Giesen, W.; Han, Q.; Hosokawa, S.; Kiswara, W.; Komatsu, T.; Lardicci, C.; Lee, K.-S.; Meinesz, A.; Nakaoka, M.; O'Brien, K.R.; Paling, E.I.; Pickerell, C.; Ransijn, A.M.A., and Verduin, J.J., 2016. Global analysis of seagrass restoration: the importance of large-scale planting. *Journal of Applied Ecology*, 53, 567–578.

Van Maren, D.S.; van Kessel, T.; Cronin, K., and Sittoni, L., 2015. The impact of channel deepening and dredging on estuarine sediment concentration. *Continental Shelf Research*, 95, 1–14.

Walter, R.K.; Rainville, E.J., and O'Leary, J.K., 2018. Hydrodynamics in a shallow seasonally low-inflow estuary following eelgrass collapse. *Estuarine, Coastal and Shelf Science*, 213, 162–175.

Wang, P. and Beck, T.M. 2012. Morphodynamics of an anthropogenically altered dual-inlet system: John's Pass and Blind Pass, west-central Florida, USA. *Marine Geology*, 291, 162–175.

Wang, P.; Beck, T.M., and Roberts, T.M. 2011. Modelling regional-scale sediment transport and medium-term morphology change at a dual-inlet system examined with the Coastal Modeling System (CMS): A case study at John's Pass and Blind Pass, West-Central Florida. *In:* Roberts, T.M.; Rosati, J.D., and Wang, P. (eds.), *Proceedings, Symposium to Honor Dr. Nicholas Kraus. Journal of Coastal Research*, Special Issue No. 59, 49–60.

Weisberg, R.H. and Zheng, L., 2006. Circulation of Tampa Bay driven by buoyancy, tides, and winds, as simulated using a finite volume coastal ocean model. *Journal of Geophysical Research*, 111, C01005.

Willmott, C.J., 1981. On the validation of models. *Physical Geography*, 2, 184–194.

Zervas, C.E. and Bourgerie, R.W., 1993. Tidal circulation. In: Zervas, C.E. (ed.), Tampa Bay Oceanography Project: Physical Oceanographic Synthesis. *NOAA Technical Report NOS OES 002*, 163p.